Electronic Supplementary Material (ESI) for ChemComm.

Solid-Solution Hexagonal $Ni_{0.5}Co_{0.5}Se$ Nanoflakes toward the Boosted Oxygen Evolution Reaction

Lei Zhu,[a,b] Yanxin Liao,[a] Yubao Jia,[a] Xin Zhang,[a] Ruguang Ma*[c] and Kuikui Wang*[a,d]

a. Institute of Materials for Energy and Environment, Laboratory of New Fiber Materials and Modern Textile, Growing Basis for State Key Laboratory, College of Materials Science and Engineering, Qingdao University, Qingdao 266071, China

b. Cancer Institute, The Affiliated Hospital of Qingdao University, Qingdao University, Qingdao 266071, China

c. State Key Laboratory of High Performance Ceramics and Superfine Microstructure, Shanghai Institute of Ceramics,Chinese Academy of Sciences, 1295 Dingxi Road, Shanghai 200050, China

d. Guangdong Provincial Key Laboratory of Advance Energy Storage Materials, South China University of Technology, Guangzhou 510640, China

Experimental Section

Synthesis of catalysts

The $Ni_{0.5}Co_{0.5}Se$ nanoflakes were synthesized by a facile hydrothermal method. Typically, elemental selenium powder (2 mmol) was dissolved in NaOH solution (2.5 M, 40 mL) with the ratio (1:3) of deionized water to thanol. $CoCl_2 \cdot 6H_2O$ (1 mmol) and $NiCl_2 \cdot 6H_2O$ (1 mmol) were dissolved in ethylene diamine tetraacetic acid solution (0.25 M, 10 mL, MEDTA). Then the above solutions were mixed, and hydrazine hydrate (7 mL) of was added dropwise. The mixture was added to Teflon liner stainless steel autoclaves and maintained in 160 °C for 20 h, and then cooled naturally. The obtained black precipitate was washed thoroughly and dried in vacuum at 80 °C for 10 h, and then the final sample was collected. For comparison, sample CoSe and NiSe nanoflakes were also prepared by the similar synthesis process.

Structure characterization

The catalysts structure and composition were characterized using powder X-ray diffraction with Cu Kα radiation (XRD, Rigaku D/MAX-2500, λ=0.15418) and X-ray photoelectron spectroscopy (ESCALAB 250 spectrometer, Thermo Scientific).The field-emission scanning electron microscopy (FE-SEM, JEOL JSM-7800F) and high-resolution transmission electron microscope (HRTEM, JEOL JEM-2100) were used to characterize the morphology and microstructure of the catalysts. And the energy-dispersive spectroscopy (EDS) elemental line scans were detected on the FE-SEM equipment. The Brunauer-Emmett-Teller (BET) method with N_2 adsorption data was

used to estimate specific surface areas in the relative pressure range of P/P_0=0.05-0.35. The Barrerr-Joyner-Halenda (BJH) model was used to calculate the pore size distributions with a Quantachrome Autosorb-IQ-MP/XR pore and surface area analyzer.

Geometry optimization and simulation

Density functional theory (DFT) calculations were performed by using Vienna Ab initio Simulation Package (VASP) to get the crystal parameters of $Ni_{0.5}Co_{0.5}Se$ and the density of states. The projector augmented wave (PAW) pseudopotentials were used to describe the interactions between core and valence electrons. The generalized gradient approximation (GGA) was applied for the electron exchange correlations. Cut-off energy was set to 400 eV for expanding the plane wave basis. The Brillouin zone was sampled with Monkhorst-Pack 2×2×2 k-points. In geometry optimization, the convergences of force and energy were set to 0.02 eV/Å and 1×10^{-5} eV, respectively.

Electrochemical measurements

All electrochemical tests were carried out and recorded by using CHI 760 electrochemical workstation in a three-electrode configuration at room temperature. For all measurements, the alkaline electrolyte was O_2-satured 1 M KOH. The working electrode was prepared as follows. The as-prepared catalyst (6 mg) was dispersed in 1 mL ethanol-water solution (740 μL ethanol, 250 μL deionized water and 10 μL Nafion solution) under sonication. Then, the suspension was sonicated for 30 min in

order to acquire a homogeneous ink. In the end, different amounts of the catalyst ink (e.g. 5, 10, 15, 20 μL) were deposited onto the glassy carbon electrode (GCE) for electrochemical measurement. And the glassy carbon electrode was mirror-polished treated and the disc area was 0.196 cm^2. A Pt foil was used as counter electrode and a saturated Hg/HgO (1 M KOH) was used as reference electrode. All the samples were firstly stabilized at 0.55 V vs. saturated Hg/HgO for 10 minutes before electrochemical measurements. Linear sweep voltammetry (LSV) was carried out from 0 to 0.8 V at a scan rate of 5 mV s^{-1}. Electrical impedance spectroscopy was measured at open circuit potential with 5 mV ac voltage amplitude in the frequency range from 100 kHz to 0.1 Hz. And chronopotentiometric measurement was recorded by setting the current density at 10 mA cm^{-2}. In this work, according to the Nernst equation ($E_{RHE} = E_{Hg/HgO} + 0.059 \times pH + 0.098$ V), the potentials were converted to a reversible hydrogen electrode (RHE) scale. And the formula η (V) = E_{RHE} –1.23 V was used to calculate the overpotential (η).

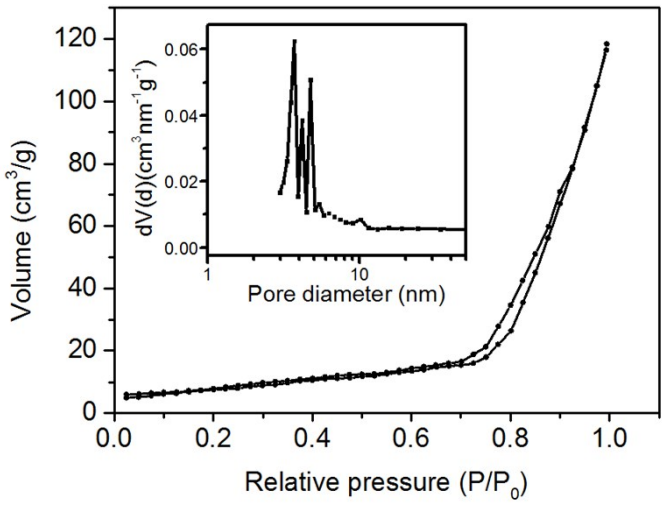

Figure S1. Nitrogen adsorption-desorption isotherms of $Ni_{0.5}Co_{0.5}Se$**.** Inset is the corresponding pore distribution curve obtained based on the Barrett-Joyner-Halenda (BJH) model.

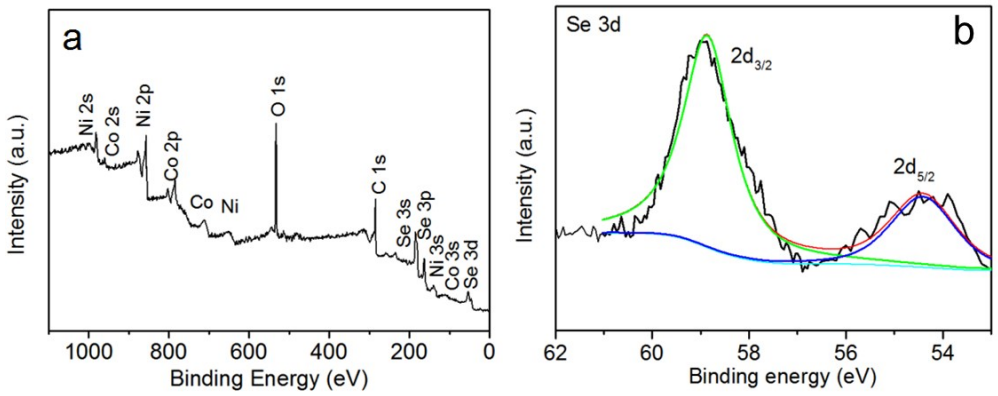

Figure S2. (a) Survey XPS spectra of $Ni_{0.5}Co_{0.5}Se$ nanoflakes, and (b) High-resolution XPS spectrum Se 3d.

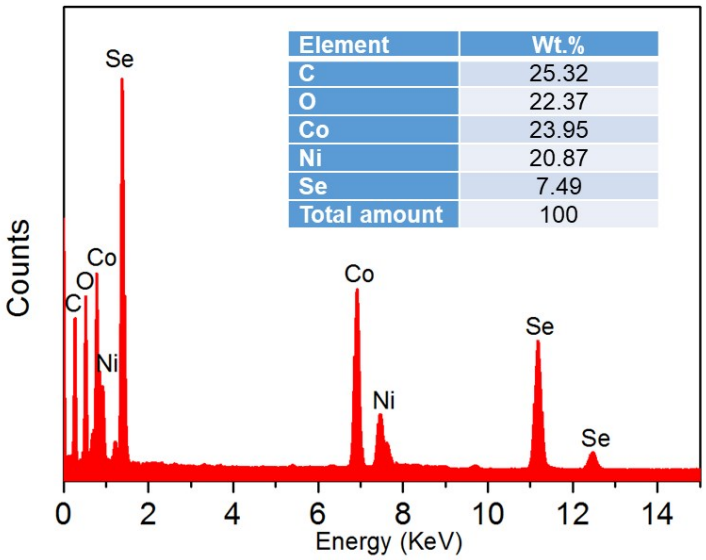

Figure S3. EDS spectra of the as-synthesized $Ni_{0.5}Co_{0.5}Se$ and the element composition of the as-synthesized $Ni_{0.5}Co_{0.5}Se$ from EDS spectra.

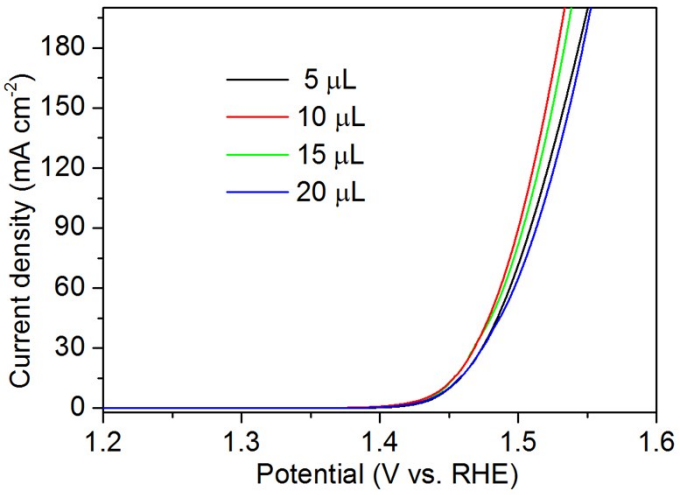

Figure S4. LSV curves for $Ni_{0.5}Co_{0.5}Se$ nanoflakes with 5, 10, 15 and 20 μL catalyst ink.

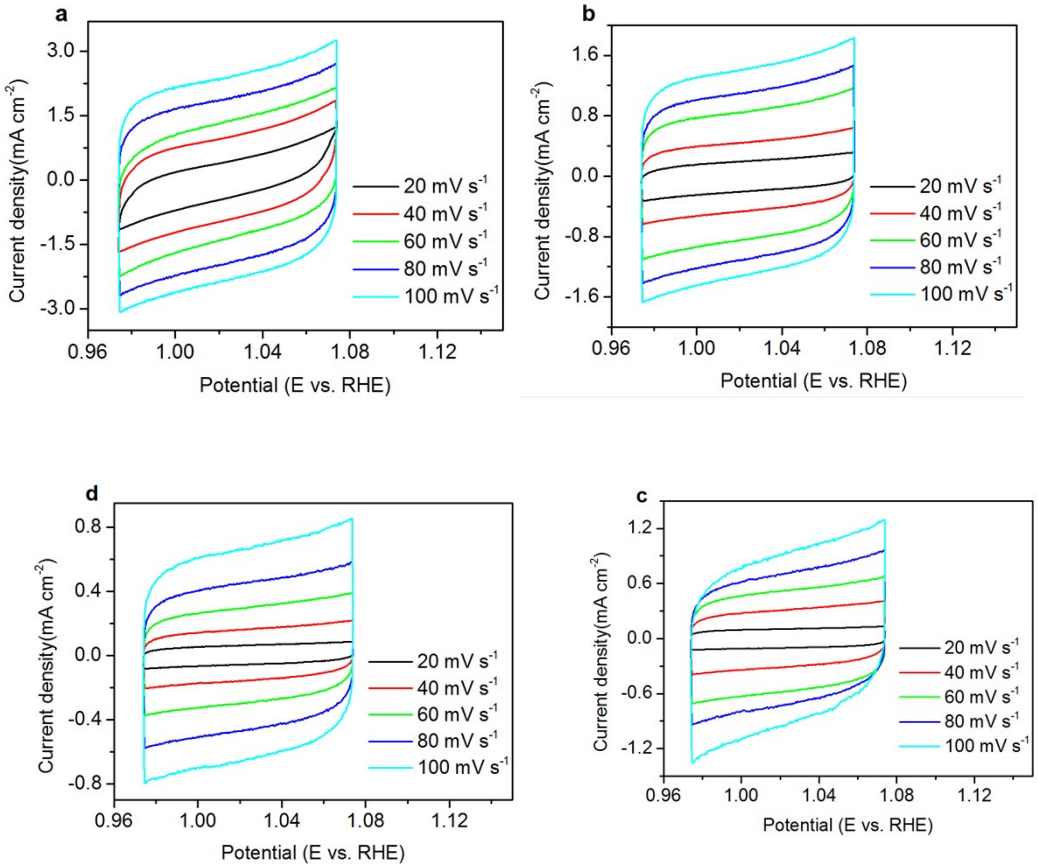

Figure S5. CV curves of current densities at 0.1 V versus scan rates of (a) $Ni_{0.5}Co_{0.5}Se$, (b) CoSe, (c) NiSe, (d) RuO_2.

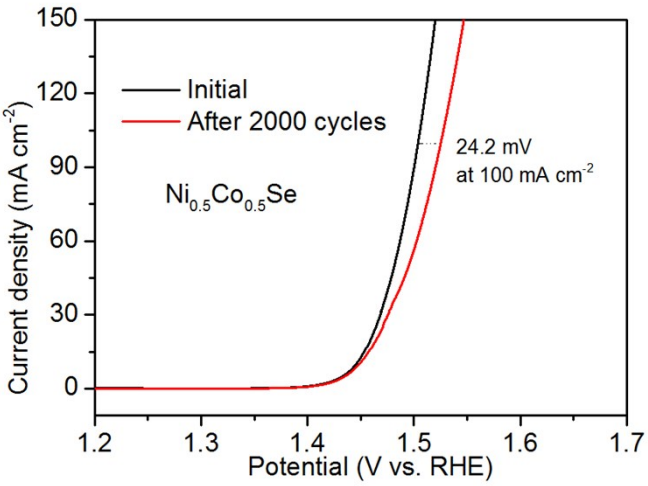

Figure S6. LSV curves of initial cycle and after the 2000th cycle.

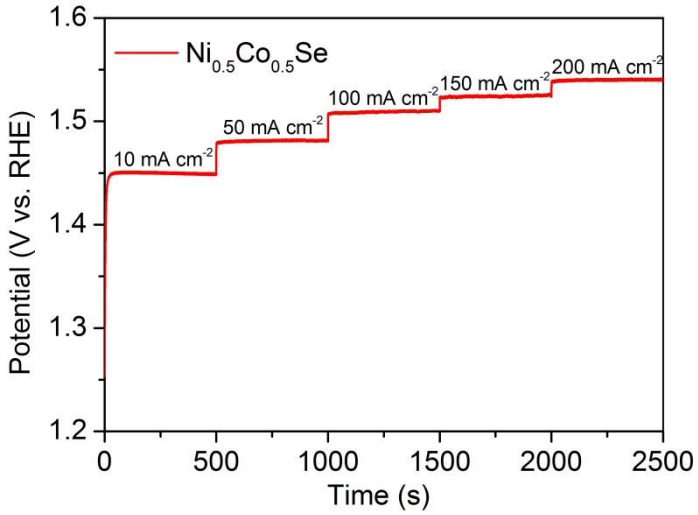

Figure S7. Chronoamperometric curve of $Ni_{0.5}Co_{0.5}Se$ in 1 M KOH at different current densities.

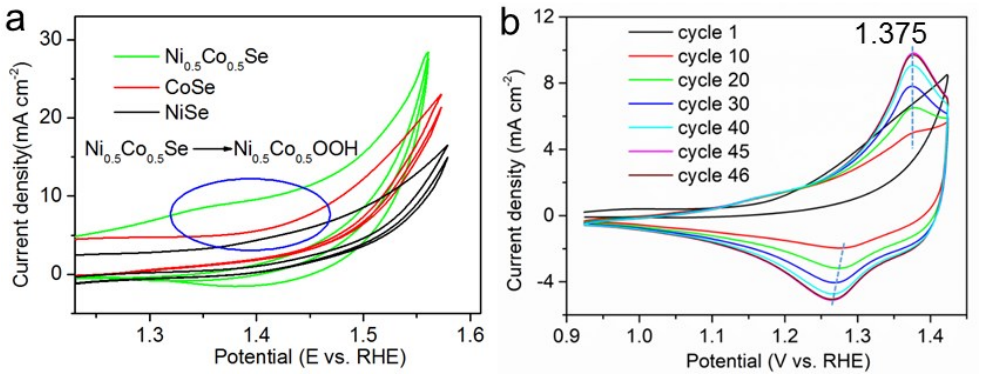

Figure S8. (a) Cyclic voltammetry activation of different catalysts. The catalysts undergo phase conversion in alkaline solution at anodic potentials. (b) Cyclic voltammetry activation of $Ni_{0.5}Co_{0.5}Se$ upon different cycles.

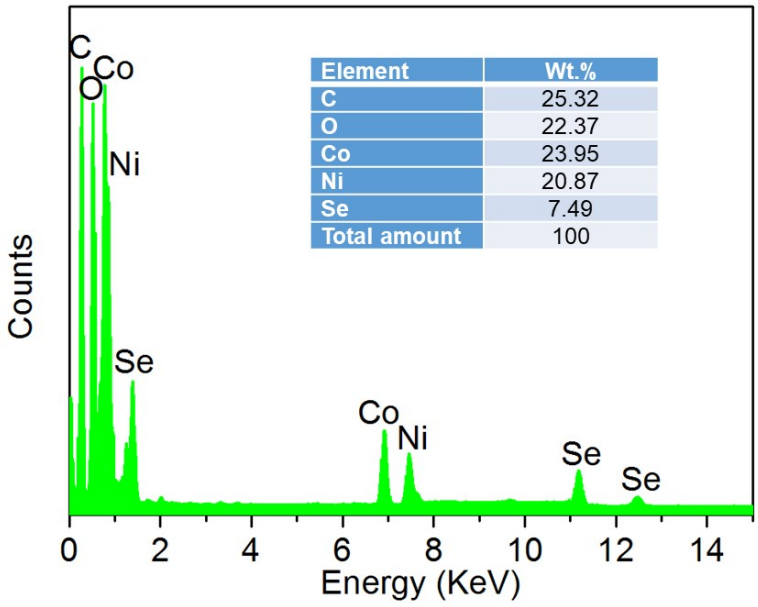

Figure S9. Energy dispersive X-ray spectroscopy pattern showed that less Se can be detected after CV stabilized, and the element composition of the as-synthesized $Ni_{0.5}Co_{0.5}Se$ after CV activation from EDS spectra.

Table S1. Comparison of the OER activity of the $Ni_{0.5}Co_{0.5}Se$ nanoflakes with other selenide-based electrocatalysts in basic condition.

Catalysts	Electrolyte	Overpotential (mV, at 10 mA cm^{-2})	Tafel slop ($mV\ dec^{-1}$)	Reference
$Ni_{0.5}Co_{0.5}Se$ nanoflakes	1.0 M KOH	216	37.08	This work
Cu_2Se@CoSe	1.0 M KOH	251	57.894	1
$CoFe_{0.7}Se_{1.7}$	1.0 M KOH	279	43.9	2
$NixFe_{1-x}Se_2$	1.0 M KOH	195	28	3
Ni-Fe-Se cages	1.0 M KOH	240	24	4
$(Ni,Co)_{0.85}Se$	1.0 M KOH	287 (at 20 mA cm^{-2})	86.75	5
$Co_{0.75}Fe_{0.25}$-Se	1.0 M KOH	246	41.4	6
CoSe nanowalls	1.0 M KOH	360	74.7	7
$CoSe_2$ nanocrystals	1.0 M KOH	430	50	8
$NiSe_2$ nanocrystals		250	38	
CoSe-0.2/NiSe-nrs/NF	1.0 M KOH	310	58.3	9
NiSe-nrs/NF		400	134	
NiSe@NiOOH/NF	1.0 M KOH	501	162	10
NiSe−$Ni_{0.85}Se$/NF	1.0 M KOH	395	98	11
$NiCo_2Se_4$	1.0 M KOH	295	53	12
Ni_3Se_2	0.3 M KOH	320	97.1	13
$CoNi_2Se_4$ nanoflake	1.0 M KOH	160	72	14
$(Ni,Co)_{0.85}Se$@NiCo-LDH	1.0 M KOH	216	77	15
$(Ni,Co)_{0.85}Se$ nanotube/CC	1.0 M KOH	255	79	
Co0.85Se nanotube/CC	1.0 M KOH	324	85	

Single-unit cell thick $CoSe_2$ NS $CoSe_2$-CeO_2	1.0 M KOH 0.1 M KOH	~350 288	64 44	16
$CoSe_2$ nanobelt CeO_2 /$CoSe_2$ nanobelt	0.1 M KOH 0.1 M KOH	460 288	66 44	17
$CoSe_2$/N-doped graphene	0.1 M KOH	366	40	18
Ultrathin $CoSe_2$ NS	0.1 M KOH	320	44	19
ECT-S/Se-$Co_{0.37}Ni_{0.26}Fe_{0.37}O$	1.0 M KOH	232	35	20
a-CoSe/Ti mesh	1.0 M KOH	292	69	21
Fe-$NiSe_2$	0.1 M KOH	268	41	22
CoSe	1.0 M KOH	295	40	23
$Ni_{1.12}Fe_{0.49}Se_2$	1.0 M KOH	227	37.87	24
$(Ni, Fe)_3Se_4$	1.0 M KOH	225	41	25
$FeSe_2$	1.0 M KOH	245		26
Ag-$CoSe_2$ NBs	0.1 M KOH	320	56	27
$Ni_{0.76}Fe_{0.24}Se$	0.1 M KOH	197	56	28
$Co_{0.13}Ni_{0.87}Se_2$/Ti	1.0 M KOH	~298 (at 50 mA cm^{-2})	94	29

References

1. X.Y. Wang, Y Zhou, Y.X. Tuo, Y. Lin, Y.G. Yan, C. Chen, Y.P. Li, J. Zhang, Electrochim. Acta 2019, 320, 134589.

2. X. Wang, Y. Zhou, M. Liu, C. Chen, J. Zhang, Electrochim. Acta 2019, 297, 197-205.

3. X. Xu, F. Song, X.L. Hu, Nat. Commun. 2016, 7, 12324.

4. J. Nai, Y. Lu, L. Yu, X. Wang, X.W. Lou, Adv. Mater. 2017, 29, 1703870.

5. K. Xiao, L. Zhou, M. F. Shao, M. Wei, J. Mater. Chem. A 2018, 6, 7585-7591.

6. K. Guo, Z. Zou, J. Du, Y. Zhao, B.F. Zhou , C.L. Xu, Chem. Commun. 2018, 54, 11140-11143.

7. X. Li, L. Zhang, M.R. Huang, S.Y. Wang, X.M. Li, H.W. Zhu, J. Mater. Chem. A. 2016, 4, 14789-14795.

8. I.H. Kwak, H.S. Im, D.M. Jang, Y.W. Kim, K. Park, Y.R. Lim, E.H. Cha, J. Park, ACS Appl. Mater. Interfaces 2016, 8, 5327-5334.

9. J.N. Du, S.J. You, X.R. Li, B. Tang, B.J. Jiang, Y. Yu, Z. Cai, N.Q. Ren, J.L. Zou, ACS Appl. Mater. Interfaces 2020, 12, 686-697.

10. C. Lei, H. Chen, J. Cao, J. Yang, M. Qiu, Y. Xia, C. Yuan, B. Yang, Z. Li, X. Zhang, L. Lei, J. Abbott, Y. Zhong, X. Xia, G. Wu, Q. He, Y. Hou, Adv. Energy Mater. 2018, 8, 1801912.

11. C.C. Hou, C.J. Wang, Q.Q. Chen, X.J. Lv, W.F. Fu, Y. Chen, Chem. Commun. 2016, 52, 14470-14473.

12. Z. Fang, L. Peng, H. Lv, Y. Zhu, C. Yan, S. Wang, P. Kalyani, X. Wu, G. Yu, ACS Nano 2017, 11, 9550-9557.

13. A. T. Swesi, J. Masud, M. Nath, Energ. Environ. Sci. 2016, 9, 1771-1782.

14. GolrokháAmin, B. Chem. Commun. 2017, 53, 5412-5415.

15. C. Xia, Q. Jiang, C. Zhao, M.N. Hedhili, H.N. Alshareef, Adv. Mater. 2016, 28, 77-85.

16. L. Liang, H. Cheng, F. Lei, J. Han, S. Gao, C. Wang, Y. Sun, S. Qamar, S. Wei, Y. Xie, Angew. Chem. Int. Ed. 2015, 54, 12004-12008.

17. Y.R. Zheng, M.R. Gao, Q. Gao, H.H. Li, J. Xu, Z.Y. Wu, S.H. Yu, Small 2015, 11, 182-188.

18. M.R. Gao, X. Cao, Q. Gao, Y.F. Xu, Y.R. Zheng, J. Jiang, S.H. Yu, ACS Nano 2014, 8, 3970-3978.

19. Y. Liu, H. Cheng, M. Lyu, S. Fan, Q. Liu, W. Zhang, Y. Zhi, C. Wang, C. Xiao, S. Wei, J. Am. Chem. Soc. 2014, 136, 15670-15675.

20. W. Chen, Y. Liu, Y. Li, J. Sun, Y. Qiu, C. Liu, G. Zhou, Y. Cui, Nano Lett. 2016, 16, 7588-7596.
21. T. Liu, Q. Liu, A.M. Asiri, Y. Luo, X. Sun, Chem. Commun. 2015, 51, 16683-16686.
22. G. Chao, S. Hu, X. Zheng, M. Gao, Y. Zheng, S. Lei, Angew. Chem. Int. Ed. 2018, 57, 1-6.
23. M. Liao, G. Zeng, T. Luo, Z. Jin, Y. Wang, X. Kou, Electrochim. Acta 2016, 194, 59-66.
24. Y. Du, G. Cheng, W. Luo, Nanoscale, 2017, 9, 6821-6825.
25. J. Du, Z. Zou, C. Liu, C. Xu, Nanoscale, 2018, 10, 5163-5170.
26. C. Panda, P.W. Menezes, C. Walter, S. Yao, M.E. Miehlich, V. Gutkin, Angew. Chem. Int. Ed. 2017, 56, 10506-10510.
27. X. Zhao, H. Zhang, Y. Yan, J. Cao, X. Li, S. Zhou, Angew. Chem. Int. Ed. 2017, 56, 328-332.
28. J. Yu, G. Cheng, W. Luo, Nano Res. 2018, 11, 2149-2158.
29. T. Liu, A.M. Asiri, X. Sun, Nanoscale, 2016, 8, 3911-3915.
30. Y.J. Qin, F.P. Wang, J. Shang, Muzaffar Iqbal, A.J. Han, X.M. Sun, H.J. Xu, J.F. Liu, J. Energy Chem. 2020, 43, 104-107.